

Journal of Materials Chemistry B

Accepted Manuscript



This is an *Accepted Manuscript*, which has been through the Royal Society of Chemistry peer review process and has been accepted for publication.

Accepted Manuscripts are published online shortly after acceptance, before technical editing, formatting and proof reading. Using this free service, authors can make their results available to the community, in citable form, before we publish the edited article. We will replace this *Accepted Manuscript* with the edited and formatted *Advance Article* as soon as it is available.

You can find more information about *Accepted Manuscripts* in the [Information for Authors](#).

Please note that technical editing may introduce minor changes to the text and/or graphics, which may alter content. The journal's standard [Terms & Conditions](#) and the [Ethical guidelines](#) still apply. In no event shall the Royal Society of Chemistry be held responsible for any errors or omissions in this *Accepted Manuscript* or any consequences arising from the use of any information it contains.

Cite this: DOI: 10.1039/c0xx00000x

www.rsc.org/xxxxxx

Cellulose-graft-poly(L-lactic acid) nanoparticles for efficient delivery of anti-cancer drugs

Lin Dai, ‡^a Tingyuan Yang, ‡^b Jing He,^a Lihong Deng,^a Jing Liu,^a Luying Wang,^a Jiandu Lei^{*a}, and Lianyan Wang^{*b}

Received (in XXX, XXX) Xth XXXXXXXXX 20XX, Accepted Xth XXXXXXXXX 20XX

DOI: 10.1039/b000000x

Cellulose based carriers have the potential of sustained release drugs, which can protect drugs and deliver them to the target site. Herein, BA-loaded cellulose-graft-poly(L-lactic acid) nanoparticles (CE-g-PLLA/BA NPs) were fabricated by employing cellulose (CE) and poly(L-lactic acid) (PLLA) as materials and betulinic acid (BA) as a model drug. Both drug-free and BA-loaded nanoparticles were spherical in shape with a uniform size of 100–170 nm. The release of BA from CE-g-PLLA/BA NPs was relatively slow. *In vitro* cytotoxicity studies with A549 and LLC cell lines suggested that CE-g-PLLA/BA NPs was slight superior to BA in antitumor activity and CE-g-PLLA NPs were non-toxic. The antitumor effect of the CE-g-PLLA/BA NPs in a mouse tumor xenograft model exhibited much better tumor inhibition efficacy and fewer side effects than that of BA, strongly supporting their use as efficient carriers for anti-cancer therapy.

1 Introduction

Polymeric amphiphiles consisting of hydrophilic and hydrophobic segments have received increasing attention for their ability to improve the efficacy of anticancer drugs owing to their small size, prolonged circulation time, and sustained drug release profile.^{1–3} In the aqueous phase, the hydrophobic cores of polymeric nanoparticles are surrounded by hydrophilic outer shells. Thus, the inner core can serve as a nano-container for hydrophobic anticancer drugs.^{4–6} Moreover, compared with other delivery systems, nanoparticles show advantages in passive tumor targeting through the leaky vasculature via the enhanced permeability and retention (EPR) effect due to their small size ranging from 10 to 200 nm, which is small enough to avoid filtration by the lung and spleen. Therefore, drug delivery using polymeric nanoparticles is an effective strategy for passive tumor targeting.^{7–10} In recent years, cellulose based graft copolymers such as cellulose acetate, cellulose acetate propionate, -butyrate, and -phthalate as well as cellulose acetates with varying degree of substitution self-assemble into regular nanoparticles.^{11, 12}

As the most important skeletal component in plants, the polysaccharide cellulose is an almost inexhaustible polymeric raw material with fascinating structure and properties.¹³ Formed by the repeated connection of d-glucose building blocks, the highly functionalized, linear stiff-chain homopolymer is characterized by its hydrophilicity, chirality, biodegradability, broad chemical modifying capacity, and its formation of versatile semicrystalline fiber morphologies. It is a promising “green” material owing to its unique properties such as nontoxicity, recyclability, and low cost. The functionalization and value-

added utilization of cellulose is always an important topic in the field of food and pharmaceutical research.¹⁴ Especially owing to their biocompatibility bearing anticancer drugs have received an increasing amount of attention. However, the application of cellulose has been hampered due to its high crystallinity, rigidity of backbone chain, and insolubility. Cellulose research and product development over the past decade is widely in the structure and chemistry of cellulose, and in the development of innovative cellulose esters and ethers for coatings, films, membranes, building materials, drilling techniques, pharmaceuticals, and foodstuffs.^{15, 16} As far as biocompatibility of biomedical polymer material is concerned, poly(L-lactic acid) (PLLA) has been choice to graft onto the backbones of cellulose. Copolymers obtained from PLLA and cellulose will combine the advantages of both, such as amphiphilic and biocompatibility. In the previous study, we successfully synthesized the cellulose-graft-poly(L-lactic acid) (CE-g-PLLA) and the degree of polymerization of poly(L-lactic acid) (DP_{PLLA}) can be well-controlled, and different DP_{PLLA} of the polymer showed different degradability.^{17, 18} Furthermore, the microstructure of polymer was investigated by TEM, which laid the foundation for the study of drug loading.

In this study, betulinic acid (BA), a hydrophobic anticancer drug was loaded into CE-g-PLLA nanoparticles (CE-g-PLLA NPs) for the sustained release and reducing side effects of free BA. BA was discovered in a National Cancer Institute drug screening program of natural plant extracts, and has been recognized to possess potent antitumor activity against ovarian carcinoma, breast, lung, and head/neck cancer.^{19–21} Until now,

clinical application of BA in cancer therapy is limited due to the very lipophilic characteristics of BA and its consequently poor solubility, relatively short half-life, and low bioavailability.²²⁻²⁴ Here, the usefulness of CE-g-PLLA NPs as a carrier of BA was evaluated by measuring its loading efficiency, drug release profile, and cytotoxicity *in vitro*. We also examined the antitumor activity of the CE-g-PLLA/BA NPs in tumor-bearing mice.

2 Experimental

2.1 Reagents and materials

Microcrystalline cellulose with polymerization degree (DP) of 255 and N-methylimidazole concentrations of 99% was provided by the J&K Chemical Reagent Co., Ltd, China. Allyl chloride with concentrations of 98% was purchased from Acros Organics, USA. 1-allyl-3-methylimidazolium chloride (AmimCl) was synthesized according to the literature.²⁵ L-lactic acid (L-LA) with a purity of 98% was purchased from A Johnson Matthey Co., Great Britain. 4-dimethylaminopyridine (DMAP) with a purity of 99.5% was provided by Haili Chemical Industry Co., Ltd. Vivaspin ultracentrifugation filters with 10 kDa MWCO were purchased from Fisher (Ottawa, ON, Canada). All other reagents were purchased from Sigma Aldrich.

Penicillin and streptomycin, Gibco Dulbecco's Phosphate-Buffered Saline (DPBS), Gibco Dulbecco's Modified Eagle's Medium (DMEM) were all bought from Invitrogen. Fetal bovine serum (FBS) was from HyClone. Cell-Counting Kit-8 (CCK-8) kit was supplied by the Dojindo Laboratories. Human lung cancer cells (A549) and murine Lewis lung carcinoma (LLC) cells were obtained from the Peking University Health Science Center (Beijing, China) and were cultured in the listed medium: A549 by RPMI 1640 with 10% FBS, 1% streptomycin-penicillin and LLC by DMEM with 10% FBS, 1% streptomycin-penicillin. All cell lines were maintained in an incubator supplied with 5% CO₂/95% air humidified atmosphere at 37 °C.

Female C57BL/6 mice, 6-7 weeks age, were purchased from Beijing HFK BIOSCIECE CO., LTD. All animal experiments were in compliance with the Institutional Ethical Committee for animal care guidelines.

2.2 Synthesis of cellulose-graft-poly(L-lactic acid) (CE-g-PLLA)

The CE-g-PLLA polymer was synthesized via ring-opening polymerization (ROP) by using DMAP as an organic catalyst in an ionic liquid AmimCl, as previously reported.¹⁷ Briefly, 4% (w/w) MCC/AmimCl solution (15 g) was first prepared by mechanical stirring at 80°C under nitrogen for 1 h in a dried Schlenk tube; then L-LA (5.4 g, 0.038 mol), DMAP (1.5 g, 0.013 mol) were added into the tube and mixed till dissolved, the tube was degassed in vacuum/N₂ in 1 h cycles (three times); finally, the reaction was kept at 90°C under nitrogen with vigorous stirring for 9 h; after cooling to room temperature, the resultant polymer was precipitated with deionized water, and then dissolved in toluene to obtain a purified graft polymer. The purified product was dried in a vacuum oven at 60°C till constant weight. The chemical structure of the synthesized CE-g-PLLA was analyzed by ¹H-NMR and ¹³C-NMR.^{17, 18}

2.3 Preparation of BA-loaded CE-g-PLLA nanoparticles (CE-g-PLLA/BA NPs)

Nanoparticles were prepared by a nanoprecipitation method as described previously with minor modification.²⁶ CE-g-PLLA (6 g) and BA (3 mg) in 0.5 mL of dry DMSO was mixed and added dropwise to a vortexing solution of normal saline in a 5.5 mL conical tube. Vortexing was maintained for 10 min after solution addition. The resulting CE-g-PLLA/BA NPs solutions were dialyzed against distilled water using a membrane with a molecular weight cutoff of 10,000 for 3 h with two exchanges of dialysate, and the supernatant was filtered through a 0.8 µm membrane and lyophilized. CE-g-PLLA NPs was similarly prepared and purified as that for CE-g-PLLA/BA NPs except adding BA. The size of the particles was determined by dynamic light scattering with a particle analyzer (Zetasizer Nano-ZS, Malvern Instruments Ltd., Malvern, UK).

2.4 Determination of critical aggregation concentration (CAC)

The CAC of CE-g-PLLA was determined by employing pyrene as a fluorescence probe.²⁷ A drug-free CE-g-PLLA solution in DPBS (2.5 mg/mL) was prepared via solvent evaporation method. A series of 2-fold dilutions was then made with CE-g-PLLA concentrations ranging from 2 to 200 mg/L. All the aqueous sample solutions obtained a final pyrene at the same concentrations of 6×10⁻⁷ M. The solutions were kept on a shaker at 37 °C for 24 h to reach equilibrium before fluorescence measurement. The fluorescence intensity of samples was measured at the excitation wavelength ranging from 240 to 360 nm and emission wavelength of 390 nm by Synergy HI Hybrid Multi-Mode Microplate Reader (Winooski, VT). Both excitation and emission bandwidths were 10 nm. From the pyrene emission spectra, the intensities at 337 nm were analyzed as a function of the polymer concentrations. The CAC was determined from the threshold concentration, where the sharp increase in pyrene fluorescence intensity was observed.

2.5 Determination of drug loading and *in vitro* drug release

CE-g-PLLA/BA NPs (20 mg/mL) was diluted into 10 mL phosphate buffered saline adjusted to pH 7.4 and incubated at 37 °C. Aliquots of 0.2 mL were removed at different time points and filtered through 0.22 µm PVDF syringe filter. The volume of solution was held constant by adding 0.2 mL phosphate buffered saline (pH 7.4) after each sampling. BA in the filter was measured by high-performance liquid chromatography (HPLC, Waters) using a reverse phase column (C18). The detection was performed by using UV detector at 210 nm, 85:15 mixture (v/v) of acetonitrile-water as a mobile phase, flow rate at 1.0 mL/min. Stability profile graph was generated by plotting the percentage of remaining starting material over a time course. The percentage was calculated on the basis of the ratio of the peak area of the sample at every 12 h vs the initial area peak. Each stability profile represents the average of two independent runs with the same sampling schedules. The standard deviation of each point is typically 2% or less. Drug loading efficiency (DLE) was calculated according to the following equation:
DLE (%) = (weight of loaded drug/weight of nanoparticles) × 100%

2.6 TEM analysis

CE-g-PLLA NPs and CE-g-PLLA/BA NPs were diluted 100 × in deionized water, and a 2 μL aliquot of solution was pipetted onto the surface of Formvar coated copper TEM grids (TedPella, Redding, CA) and allowed to air-dry. Analysis was performed on a JEM-100CXa TEM at an acceleration voltage of 100 kV.

2.7 Hemolysis Assay

The hemolytic activity of polymer solutions was investigated as reported earlier.^{28, 29} Briefly, fresh blood samples were collected through cardiac puncture from rats. Ten milliliters of blood was added with EDTA-Na₂ immediately to prevent coagulation. The red blood cells (RBCs) were collected by centrifugation at 1500 rpm for 10 min at 4 °C. After washing in ice-cold DPBS until the supernatant was clear, erythrocytes were diluted at a final concentration of 5 × 10⁸ cells/mL in ice-cold DPBS. 1 mL CE-g-PLLA NPs, CE-g-PLLA/BA NPs or PEI_{25K} solution (1 mg/mL and 0.1 mg/mL) was mixed with 1 mL erythrocyte suspension. DPBS and 1% Triton X-100 in DPBS were used as negative control (0% lysis) and positive control (100% lysis), respectively. Samples were incubated for 1 h at 37 °C under constant shaking. After centrifugation at 1500 rpm for 10 min at 4 °C, supernatant was analyzed for hemoglobin release at 541 nm using an infinite M200 microplate spectrophotometer (Tecan, Switzerland). Hemoglobin release was calculated as $(OD_{\text{sample}} - OD_{\text{negative control}}) / (OD_{\text{positive control}} - OD_{\text{negative control}}) \times 100\%$. Hemolysis was determined from three independent experiments.

2.8 In vitro cell cytotoxicity

CCK-8 assay was used for cell viability evaluation of different samples.³⁰ Briefly, two types of lung cancer cells LLC and A549 cells were respectively seeded at a density of 3 × 10³ and 4 × 10³ cells/well in 180 μL culture medium within a 96-well plate (Corning, USA) and incubated overnight. Then, the cells were treated with various samples (BA, CE-g-PLLA, and CE-g-PLLA/BA) at 37 °C in a humidified incubator with 5% CO₂ for 72 h, where the samples of the BA were dissolved in dimethylsulfoxide (Merck, Darmstadt, Germany) and diluted into tissue culture medium before assay and BA dose ranged from 2.5 to 500 μg/mL. 20 μL of CCK-8 solution was added to each well of the plate and incubated for another 1 h at 37 °C. The absorbance at 450 nm was measured by infinite M200 microplate spectrophotometer. Percent viability was normalized to cell viability in the absence of the samples. The IC₅₀ was calculated as polymer concentrations which inhibited growth of 50% of cells relative to non-treated cells according to Unger et al.³¹ IC₅₀ was calculated using the Boltzmann sigmoidal function from Origin[®] 8.6 (OriginLab, Northampton, USA). Data are representative of three independent experiments.

2.9 In vivo efficacy studies

Subcutaneous tumor xenograft models were established in the right axillary flank region of female C57BL/6 mice (6-7 wk) by injecting 1 × 10⁶ LLC cells in 200 μL DMEM medium per mouse. Treatments were initiated when tumors reached an average volume of 100 to 150 mm³, and this day was designated as day 0. On day 0, these mice were randomly divided into 3 groups (n = 6) and administered intravenous injection with PBS (control), free BA (10 mg/kg), and CE-g-PLLA/BA (10 mg BA/kg), respectively, on days 1, 3, 5, 7, and 9. It is important to note that

the concentrations of CE-g-PLLA/BA NPs stated in this article refer to BA equivalents. For example, a dose of 10 mg/kg of CE-g-PLLA/BA (DP_{PLLA} = 3.98) means that the dose contains 10 mg/kg of BA and 38.94 mg/kg of whole nanoparticles, assuming that the loading of BA in the whole nanoparticles is 25.68%. In the observation phase, mice were monitored for tumor sizes and body weights every other day. Tumor volume was calculated using the formula: $(L \times W^2) / 2$, where L is the longest and W is the shortest tumor diameter (millimeter).³²⁻³⁴ Relative tumor volume (RTV) was calculated at each measurement time point (where RTV was equal to the tumor volume at a given time point divided by the tumor volume prior to initial treatment). For efficacy studies, the percentage of tumor growth inhibition (%TGI) was calculated using the following formula: $[(C - T) / C] \times 100$, where C is the mean tumor volume of the control group at a specified time and T is the mean tumor volume of the treatment group at the same time. To monitor potential toxicity, we measured the weight of each mouse. For humane reasons, animals were killed and regarded as dead if the implanted tumor volume reached to 5000 mm³ or at the end of the experiment (> 6 wk). To further evaluate the hematological toxicity of the nanoparticles, we collected 200 μL blood of each mouse after final administration to test the white blood cell number (WBC) using a hematology analyzer (MEK-7222K, Nihon Kohden Celltac E).

2.10 Detection of allergic reaction

Toxic side-effects of the current chemotherapeutic drugs are often causing a severe reduction in the quality of life, so the detection of allergic reaction is very necessary and important. During the early development of drugs, type I hypersensitivity is the most common type of the hypersensitivity reaction. Some of the natural anti-cancer drugs, such as paclitaxel, docetaxel, and teniposide cyclosporine, were usually associated with a high incidence of the type I hypersensitivity reaction. It has been demonstrated that IgE antibodies play an important part in mediating type I hypersensitivity responses. We thus selected IgE levels as the parameter for rapid evaluation of type I hypersensitivity reactions. Three groups of tumor bearing mice (26-28 g, n = 6) were used in allergy testing studies of BA in two samples (control, BA, and CE-g-PLLA/BA). The two samples were administered via tail intravenous injection every two days at the BA dose of 10 mg/kg body weight. After administration with different samples for 10 days, orbit blood of mice in different groups was collected and centrifuged. Serum samples were analyzed according to the procedure of mouse IgE ELISA.

2.11 Statistical analysis.

All experiments in this study were performed at least three times, and the data were expressed as the means standard deviation (SD). Statistical analyses were performed by analysis of variance (ANOVA). In all analyses, $p < 0.05$ was taken to indicate statistical significance.

3 Results and Discussion

3.1 Synthesis of CE-g-PLLA copolymers

Cellulose-hydrophilic polymer conjugates have been extensively investigated and are relatively easy to synthesize in solution by a “grafting onto” approach.³⁵ In this study, the copolymer made of

cellulose and hydrophobic PLLA was successfully synthesized according to our previous report.^{17, 18} Although cellulose-hydrophobic polymer is expected to have interesting additional functionalities due to their amphiphilic molecular structures, however, to our knowledge, the synthesis of cellulose-hydrophobic polymer conjugates has been recognized to be difficult mainly because of the insolubility of cellulose polymer in general organic solvents. In this study, the conjugate made of cellulose and hydrophobic PLLA was successfully synthesized. Cellulose was dissolved in AmimCl at 90 °C at a concentration of 4% (w/w). DMAP and L-LA were added to conduct the ring opening polymerization to form the CE-g-PLLA copolymer. ¹H-NMR and ¹³C-NMR were used to confirm the chemical composition of the copolymer as our previous report.^{17, 18} The DP of PLLA in the copolymer was varied from 3.15 to 3.98 as determined by ¹H-NMR, depending on the feed ratio of L-LA to cellulose. These values indicate that the attachment of PLLA chains to the cellulose increased the size of the macromolecule.

3.2 Nanoprecipitation of CE-g-PLLA/BA NPs

We have encapsulated BA as a model chemotherapy drug into the CE-g-PLLA NPs. Betulinic acid is a kind of hydrophobic drug which can be loaded into the hydrophobic core of the nanoparticles due to the PLLA hydrophobic core, whereas the hydrophilic part came from the water-soluble blocks of cellulose immersed in the water to formulate the outer shell of composite core-shell nanoparticles.³⁶⁻³⁹ The copolymer in DMSO (2.5 mg/mL) was injected into a phosphate buffered saline solution (pH 7.4) to precipitate nanoparticles. As the DP of PLLA increased from 3.15 to 3.61 to 3.98, the average size of the blank and BA-loaded nanoparticles decreased from 130.36 to 120.28 to 105.32 nm and 176.43 to 160.38 to 155.16 nm (Table 1), respectively, as determined by transmission electron microscopy (TEM) and dynamic light scattering (DLS). The results showed that the drug-loaded nanoparticles exhibited bigger spherical shape than the blank ones (Fig. 1A and 1B). Moreover, the DP of PLLA could be used to control the nanoparticle size (Table 1) which allowed us to achieve optimal pharmaceutical properties of the nanoparticles. The results suggested that in aqueous solution aggregates were formed with high DP of PLLA. When the DP was 3.98, the size of nanoparticles was smaller with better dispersion. The small size of nanoparticle system suggested its potential for effective tumor targeting *in vivo*.⁴⁰

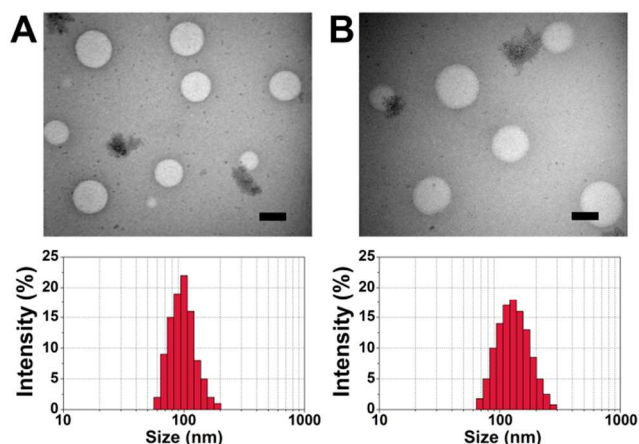


Fig. 1 TEM images and particle size distribution of CE-g-PLLA NPs (A) and CE-g-PLLA/BA NPs (B). The spherical nanoparticles with the diameter of around 100 nm were observed. The drug loading ratio was 25.68%. Scale bars were 100 nm.

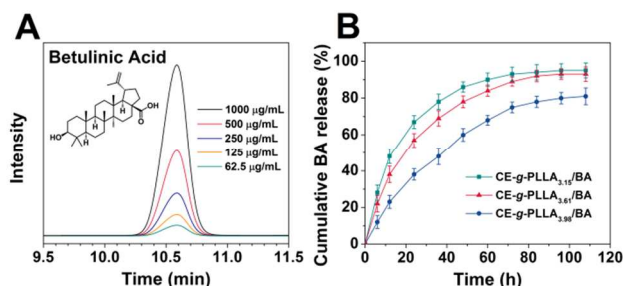


Fig. 2 Drug release of CE-g-PLLA/BA NPs in PBS pH 7.4 at 37 °C (A) measured by HPLC using UV detector at 210 nm. The presence of free BA was monitored as a function of time (B).

Drug loading efficiency (DLE) of CE-g-PLLA/BA NPs was determined by HPLC using UV detector at 210 nm (Fig. 2A) and the drug cumulative release and DLE results were shown in Fig. 2B and Table 1. When the DP of the PLLA was increased from 3.15 to 3.61 to 3.98, the DLE was increased from 18.74 to 20.32 to 25.68 wt%. The study suggested that BA encapsulated with CE-g-PLLA NPs revealed an initial burst. The initial burst release of BA from the nanoparticles was credited to BA molecules located within the shell or at the core and shell interface of the nanoparticle. The drug release equilibrium was reached after 72 h. Furthermore, an initial burst in release may be attributed to balancing the equilibrium between the inside and outside release settings. The slow release of the drug from the CE-g-PLLA NPs could be attributed to the hydrophobic-hydrophobic interactions between the BA molecules and the hydrophobic PLLA inner shell of the nanoparticles.³⁷ As shown in Fig. 2B, the CE-g-PLLA_{3.98} NPs showed more stable BA release with lower initial burst release. Therefore, the CE-g-PLLA_{3.98}/BA NPs with a 25.68 wt% loading efficiency were chosen for the following *in vitro* and *in vivo* anti-tumor activity assay.

Table 1. Particle size and drug loading efficiency of CE-g-PLLA/BA NPs

| nanoparticle | Blank NPs size (nm) | BA-loaded NPs size (nm) | DLE (wt %) |
|---------------------------|---------------------|-------------------------|--------------|
| CE-g-PLLA _{3.15} | 130.36 ± 7.28 | 176.43 ± 10.25 | 18.74 ± 1.76 |
| CE-g-PLLA _{3.61} | 120.28 ± 6.73 | 160.38 ± 9.57 | 20.32 ± 1.98 |
| CE-g-PLLA _{3.98} | 105.32 ± 6.52 | 135.16 ± 9.16 | 25.68 ± 2.03 |

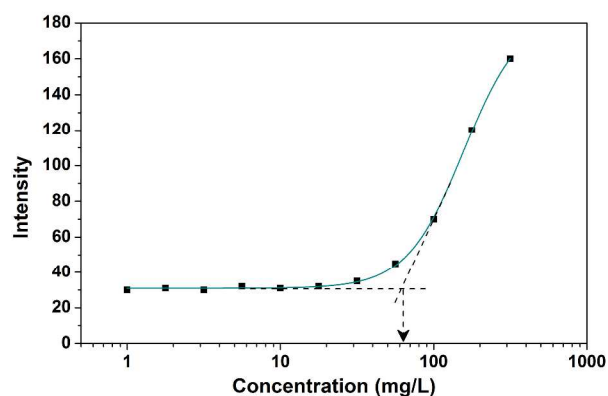


Fig. 3 CAC measurement of the CE-g-PLLA_{3.98} using pyrene as a hydrophobic fluorescence probe. The fluorescence intensity of pyrene

was collected at the excitation wavelength of 337 nm and the emission wavelength of 390 nm. The fluorescence intensity was plotted as a function of logarithmic concentration of CE-g-PLLA_{3.98} nanoparticles, [pyrene] = 6×10^{-7} mol/L. Values reported are the means \pm SD for triplicate samples.

3.3 CAC measurements

Fig. 3 showed the results of CAC measurements using pyrene as a fluorescence probe. Upon incorporation into the nanoparticles, the fluorescence intensity of pyrene increases substantially at the concentrations of nanoparticles above the CAC. On the basis of the partition of the pyrene, the CAC of CE-g-PLLA could be obtained by plotting the fluorescence intensity versus logarithm concentrations of the polymer. The CAC of CE-g-PLLA was determined from the crossover point at the low concentrations range. The CAC of the CE-g-PLLA copolymer was 64.8 μ g/mL, which is similar to most reported nanoparticles delivery systems. As CE-g-PLLA NPs was stable at the CAC, it is probable that these particles will remain stable at high dilution in biological systems. For example, in a 27 g mouse model treated at 10 mg/kg BA, 200 μ L of CE-g-PLLA/BA NPs administered i.v. (5 mg/mL CE-g-PLLA/BA NPs) would be diluted in \sim 2 mL blood volume to 2.5 mg/mL CE-g-PLLA/BA NPs. Considering the scenario when 90% of particles are out of circulation, the concentration of CE-g-PLLA/BA NPs would be still well above CAC. Moreover, CE-g-PLLA shows a good stability in our previously study (the weight loss after 24 h: 9.9%, after 2 weeks: 19.8% in PBS pH 7.4).¹⁶

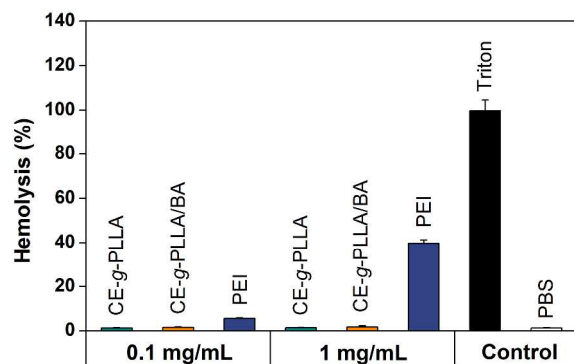


Fig. 4 *In vitro* hemolysis assay of CE-g-PLLA and CE-g-PLLA/BA NPs compared to PEI_{25K} and Triton X-100 measured at 541 nm. Values are reported as the mean \pm SD for triplicate samples.

3.4 Hemolysis study

Detrimental interaction of nanoparticles with blood constituents such as RBCs must be avoided when these nanoparticles are

injected into the blood circulation as a carrier for drug delivery.²⁹ Erythrocytes were incubated with two concentrations of polymer as 1 mg/mL and 0.1 mg/mL, for 1 h at 37 °C. Hemolysis was evaluated by measuring the amount of hemoglobin released in the supernatant at 541 nm (Fig. 4). Triton X-100 as positive control, which induced full hemoglobin release. CE-g-PLLA/BA NPs at concentrations of 1 mg/mL and 0.1 mg/mL showed a comparable hemoglobin release to blank values (<5%), which was significantly lower than similar concentrations of PEI_{25K}, a cationic polymer known to have significant hemolytic effect. Despite BA was cytotoxic to the RBCs in a previous study,⁴¹ CE-g-PLLA/BA NPs have been released little BA during the short incubation period, suggesting the excellent safety of CE-g-PLLA/BA NPs.

3.5 *In vitro* cytotoxicity

To ensure the effective of the drug delivery before their entry into human application, *in vitro* cytotoxicity should be considered upfront.^{42,43} To examine the cytotoxicity of CE-g-PLLA/BA NPs, a CCK-8 assay was conducted after incubating cells treated with different formulations. The response of two cell lines (A549 and LLC) was tested *in vitro* by seeding the cells and exposed to BA in a 10% v/v DMSO solution containing BA or CE-g-PLLA/BA NPs with the same drug concentrations. Empty nanoparticles were used as control. Cells were exposed to drug for 24, 48 or 72 h. Analysis of *in vitro* cytotoxicity measurements showed that BA (500 μ g/mL) induced cell death which was dependent upon length of incubation. As shown in Fig. 5A and 5B, the time-dependent cytotoxic effect of the CE-g-PLLA/BA NPs was evident, which indicated that 45% A549 and 40% LLC survival after 24 h, 18% A549 and 23% LLC survival after 48 h and 10% A549 and 12% LLC survival after 72 h at 500 μ g/mL (equivalent to native BA). The drug release from the CE-g-PLLA/BA NPs when incubated with cells, is possibly from the diffusion of drug molecules in the nanoparticles and the degradation of nanoparticles, which is the main mechanism of drug release observed for polymer nanoparticles.⁴⁴ To compare the potency of the CE-g-PLLA/BA NPs, the concentrations of drug which killed 50% of the cells (IC₅₀) were estimated from survival curves as shown in Fig. 5C and 5D, obtained from replicate experiments. The IC₅₀ of CE-g-PLLA/BA NPs was less than free drug. The encapsulation of BA into the nanoparticles resulted in remarkable improvements of the anti-tumor activities. Around 100% cell survival was observed for cells treated with different concentrations of empty nanoparticles, which suggested excellent biocompatibility.

Cite this: DOI: 10.1039/c0xx00000x

www.rsc.org/xxxxxx

PAPER

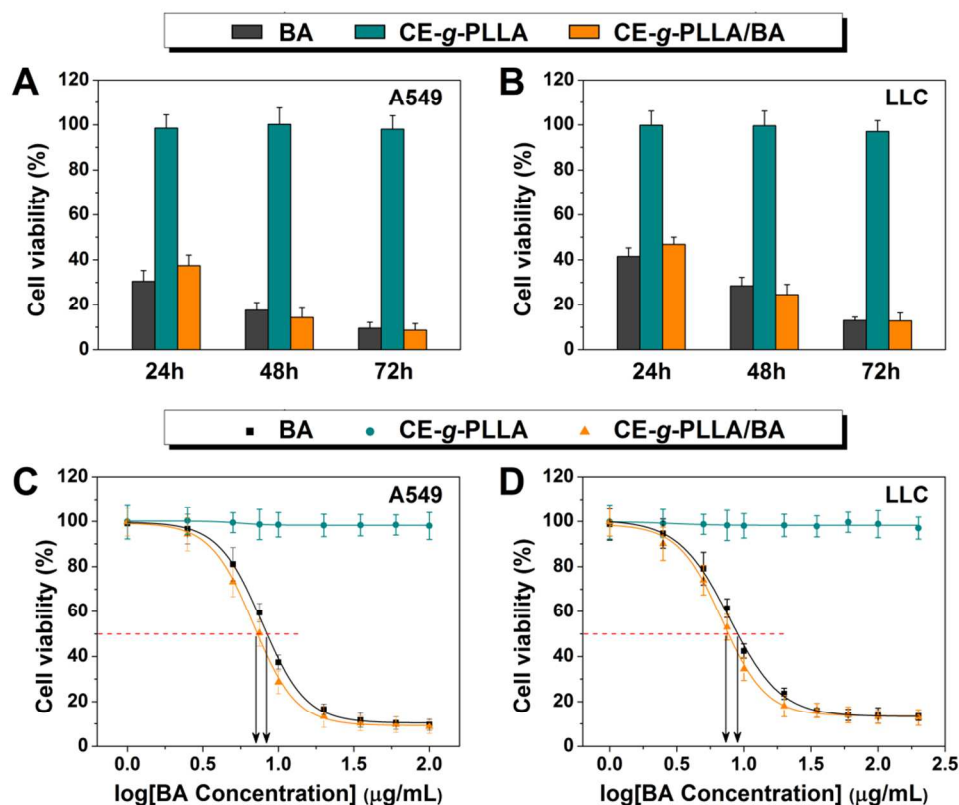


Fig. 5 Cellular cytotoxicity of BA, CE-g-PLLA NPs, and CE-g-PLLA/BA NPs in A549 and LLC cells. Cell viability of A549 (A) and LLC (B) cells treated with 500 µg/mL of BA and CE-g-PLLA/BA NPs (equivalent to native BA) was measured by CCK-8 assay (n=3, error bars represent standard deviation). CCK-8 assay of BA and CE-g-PLLA/BA NPs with different concentrations in A549 (C) and LLC (D) cell lines (n=3, error bars represent standard deviation).

Table 2. LLC Xenograft Model: Efficacy Comparison

| compound | mean TV±SD (mm ³) ^a | RTV ^a | TGI(%) ^a |
|------------------|--|------------------|---------------------|
| control | 4450 ± 1900 | 35.0 ± 15.6 | 0 |
| BA | 2368 ± 1382 | 18.5 ± 10.8 | 46.7 |
| CE-g-PLLA/BA NPs | 897 ± 400 | 6.5 ± 2.9 | 79.8 |

^a Mean tumor volume (TV), relative tumor volume (RTV), and percentage of tumor growth inhibition (% TGI) data were taken at day 20. (By day 20, a significant percentage of control animals were euthanized due to excess tumor burden.)

3.6 *In vivo* study

The results described above gave us great confidence to evaluate the anticancer effectiveness of BA formulations in a mouse tumor xenograft model. We tested the *in vivo* anti-tumor efficiency of CE-g-PLLA/BA NPs by subcutaneous inoculation of LLC cells into mice with. Treatment with BA or CE-g-PLLA/BA NPs given

as multiple doses [every 2 d (q2d) × 5] were initiated when tumors reached an average volume of 100 to 150 mm³. The results showed that, the effectiveness of the CE-g-PLLA/BA NPs was significantly better than free BA. Multiple-dose treatment of CE-g-PLLA/BA NPs caused 79.8% TGI (on day 20). In contrast, multiple-dose free BA treatment resulted in 46.7% TGI (Fig. 6A and 6C, Table 2). No significant changes in body weight were noticed in all treatment groups compared to control group (Fig. 6B). When using the BA-encapsulated CE-g-PLLA NPs for *in vivo* anti-tumor therapy, two effects are anticipated to increase the uptake of the drug-loaded nanoparticles by cancerous cells: (1) the EPR effect of solid tumors would allow more drug-loaded nanoparticles to be accumulated in the tumor tissue;^{7,8} (2) drug-loaded nanoparticles can increase the solubility of the drug.⁴⁵

Cite this: DOI: 10.1039/c0xx00000x

www.rsc.org/xxxxxx

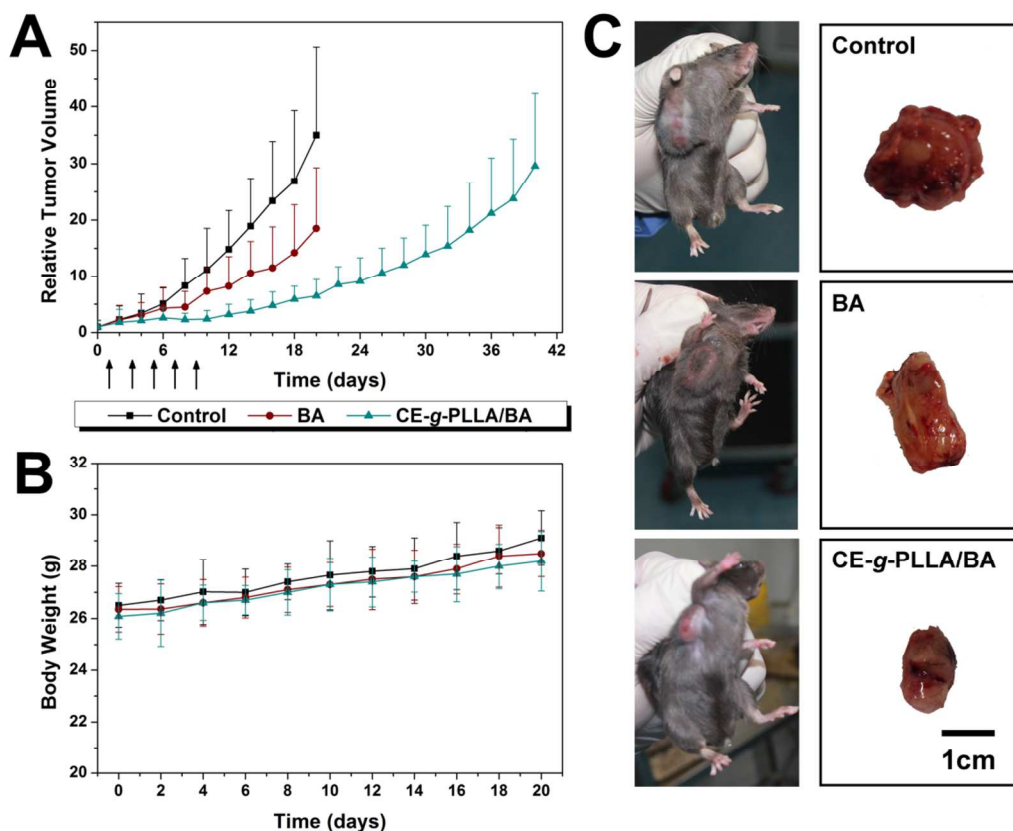


Fig. 6 Antitumor efficacy of BA and CE-g-PLLA/BA NPs in the subcutaneous mouse model of LLC. (A) Relative tumor volumes of mice during treatment with different groups. (B) Body weight after administration. (C) Tumor photographs from each treatment group excised on day 20.

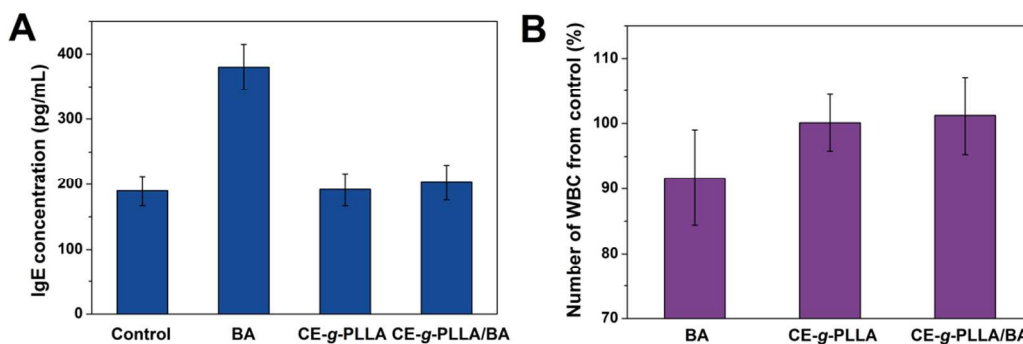


Fig. 7 Subacute toxicities of different groups were reflected by IgE levels (A) and the WBC change (B) of mice. Data as means \pm S.E.; $n = 6$.

3.7 Evaluation of the Side Effects

Although CE-g-PLLA/BA NPs showed significant therapeutic effects *in vivo*, whether these nanoparticles had non-negligible adverse effects remained a critical issue. During its early

development, type I hypersensitivity is the most common type of the hypersensitivity reaction. Some of the natural anti-cancer drugs, such as paclitaxel, docetaxel, and teniposide cyclosporine, were usually associated with a high incidence of the type I

hypersensitivity reaction. It has been demonstrated that IgE antibodies play an important part in mediating type I hypersensitivity responses. We thus selected IgE levels as the parameter for rapid evaluation of type I hypersensitivity reactions.

The blood IgE levels of mice in different groups (BA, CE-g-PLLA, and CE-g-PLLA/BA NPs) were shown in Fig. 7A. Mice treated with BA displayed a higher IgE level than the control group, which might be ascribed to the bad water solubility. As expected, no significant change of IgE level was observed in the CE-g-PLLA and CE-g-PLLA/BA NPs groups, which explored the idea that the use of these nanoparticles could reduce the risk of hypersensitivity reactions substantially. The blood of mice after treatment with different BA formulations was also collected to test the WBC count, which is often used as an indicator of hematologic toxicity. The total WBC count of mice treated with BA showed a little decrease over the normal group (Fig. 7B). No discernible decreases in WBC number of the mice treated with CE-g-PLLA and CE-g-PLLA/BA NPs were observed, indicating that the nanoparticles designed in this study could avoid severe hematotoxicity.

4 Conclusions

In summary, we had developed a cellulose-polymer hybrid nanoparticle platform consisting of a hydrophobic polymeric core of PLLA and a hydrophilic shell of cellulose. It is known that PLLA and cellulose are all biocompatible and biodegradable *in vivo*. In the *in vitro* and *in vivo* study, we demonstrated that empty CE-g-PLLA NPs showed good biocompatibility and no toxicity to cells or mice. As an example of this type of drug delivery vehicles, compared with free drug formulation, the CE-g-PLLA/BA NPs exhibited enhanced anti-tumor activity both *in vitro* and *in vivo*.

Acknowledgements

This work was supported by the Fundamental Research Funds for the Central Universities (No. 200-1244951), the China State Forestry Administration 948 Project (No. 2014-4-35), National Science Foundation of Beijing, China (Grant No. 2142024) and the National Natural Science Foundation of China (No. 20976179).

Notes and references

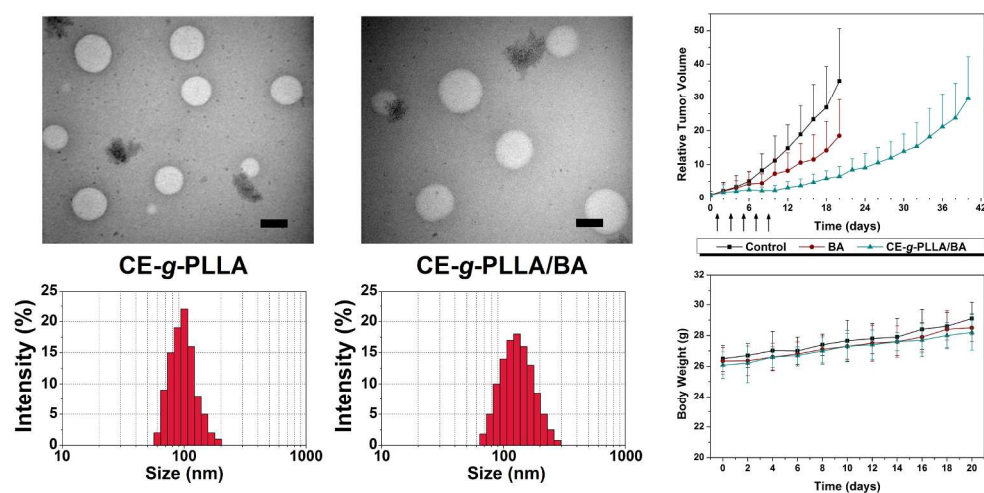
^a MOE Key Laboratory of Wooden Material Science and Application, Beijing Forestry University, Beijing 100083, P. R. China. Fax: +86 62336061; Tel: +86 1062337251; E-mail: ljd2012@bjfu.edu.cn

^b National Key Lab of Biochemical Engineering, Institute of Process Engineering, Chinese Academy of Sciences, Beijing, 100190, PR China. Fax/Tel: 8610-82544931; E-mail: wanglianyan@home.ipe.ac.cn

‡ Both Lin Dai and Tingyuan Yang contributed equally to this study.

- Meng, W. Huang, D. Wang, X. Huang, X. Zhu and D. Yan, *Biomacromolecules*, 2013, **14**, 2601-2610.
- R. P. Singh, J.-W. Choi, A. Tiwari and A. C. Pandey, in *Biosensors Nanotechnology*, John Wiley & Sons, Inc., 2014, pp. 141-197.
- S. K. Shukla and A. Tiwari, in *Responsive Materials and Methods*, John Wiley & Sons, Inc., 2013, pp. 357-375.
- T. K. Endres, M. Beck-Broichsitter, O. Samsonova, T. Renette and T. H. Kissel, *Biomaterials*, 2011, **32**, 7721-7731.
- R. Ghosh Chaudhuri and S. Paria, *Chemical Reviews*, 2011, **112**, 2373-2433.
- C. Zhu and Q. Chen, in *Advanced Healthcare Materials*, John Wiley & Sons, Inc., 2014, pp. 439-464.
- H. Maeda, J. Wu, T. Sawa, Y. Matsumura and K. Hori, *Journal of Controlled Release*, 2000, **65**, 271-284.
- H. Maeda, *Journal of Controlled Release*, 2012, **164**, 138-144.
- R. P. Singh, J. W. Choi, A. Tiwari and A. C. Pandey, in *Biomedical Materials and Diagnostic Devices*, John Wiley & Sons, Inc., 2012, pp. 215-262.
- M. Tanwar, J. Meena and L. S. Meena, in *Advanced Biomaterials and Biodevices*, John Wiley & Sons, Inc., 2014, pp. 487-521.
- X. Li, K. Y. Wang, B. Helmer and T.-S. Chung, *Industrial & Engineering Chemistry Research*, 2012, **51**, 10039-10050.
- C. Huang, S. J. Soenen, E. van Gulck, G. Vanham, J. Rejman, S. Van Calenbergh, C. Vervaet, T. Coenye, H. Verstraelen, M. Temmerman, J. Demeester and S. C. De Smedt, *Biomaterials*, 2012, **33**, 962-969.
- R. J. Moon, A. Martini, J. Nairn, J. Simonsen and J. Youngblood, *Chemical Society Reviews*, 2011, **40**, 3941-3994.
- F. A. Aouada, M. R. de Moura, W. J. Orts and L. H. Mattoso, *Journal of agricultural and food chemistry*, 2011, **59**, 9433-9442.
- D. Klemm, B. Heublein, H.-P. Fink and A. Bohn, *Angewandte Chemie International Edition*, 2005, **44**, 3358-3393.
- J. Kim, S. Yun and Z. Ounaies, *Macromolecules*, 2006, **39**, 4202-4206.
- L. Dai, D. Li and J. He, *Journal of Applied Polymer Science*, 2013, **130**, 2257-2264.
- L. Dai, L.-Y. Wang, T.-Q. Yuan and J. He, *Polymer Degradation and Stability*, 2014, **99**, 233-239.
- X. Liu, I. Jutooru, P. Lei, K. Kim, S. O. Lee, L. K. Brents, P. L. Prather and S. Safe, *Molecular cancer therapeutics*, 2012, **11**, 1421-1431.
- L. Li, Y. Du, X. Kong, Z. Li, Z. Jia, J. Cui, J. Gao, G. Wang and K. Xie, *Clinical cancer research : an official journal of the American Association for Cancer Research*, 2013, **19**, 4651-4661.
- H. Ehrhardt, S. Fulda, M. Fuhrer, K. M. Debatin and I. Jeremias, *Leukemia*, 2004, **18**, 1406-1412.
- E. Pisha, H. Chai, I.-S. Lee, T. E. Chagwedera, N. R. Farnsworth, G. A. Cordell, C. W. W. Beecher, H. H. S. Fong, A. D. Kinghorn, D. M. Brown, M. C. Wani, M. E. Wall, T. J. Hieken, T. K. Das Gupta and J. M. Pezzuto, *Nat Med*, 1995, **1**, 1046-1051.
- H.-J. Jeong, H.-B. Chai, S.-Y. Park and D. S. H. L. Kim, *Bioorganic & medicinal chemistry letters*, 1999, **9**, 1201-1204.
- F. Li, R. Goila-Gaur, K. Salzwedel, N. R. Kilgore, M. Reddick, C. Matallana, A. Castillo, D. Zoumplis, D. E. Martin, J. M. Orenstein, G. P. Allaway, E. O. Freed and C. T. Wild, *Proceedings of the National Academy of Sciences*, 2003, **100**, 13555-13560.
- J. Wu, J. Zhang, H. Zhang, J. He, Q. Ren and M. Guo, *Biomacromolecules*, 2004, **5**, 266-268.
- M. J. Ernsting, W.-L. Tang, N. MacCallum and S.-D. Li, *Bioconjugate chemistry*, 2011, **22**, 2474-2486.
- S. B. La, T. Okano and K. Kataoka, *Journal of pharmaceutical sciences*, 1996, **85**, 85-90.
- J. Nguyen, T. W. J. Steele, O. Merkel, R. Reul and T. Kissel, *Journal of Controlled Release*, 2008, **132**, 243-251.
- R. Reul, J. Nguyen and T. Kissel, *Biomaterials*, 2009, **30**, 5815-5824.
- W. Wei, P.-P. Lv, X.-M. Chen, Z.-G. Yue, Q. Fu, S.-Y. Liu, H. Yue and G.-H. Ma, *Biomaterials*, 2013, **34**, 3912-3923.
- F. Unger, M. Wittmar and T. Kissel, *Biomaterials*, 2007, **28**, 1610-1619.
- K. Kim, J. H. Kim, H. Park, Y. S. Kim, K. Park, H. Nam, S. Lee, J. H. Park, R. W. Park, I. S. Kim, K. Choi, S. Y. Kim, K. Park and I. C. Kwon, *Journal of controlled release : official journal of the Controlled Release Society*, 2010, **146**, 219-227.

33. M. J. Ernesting, M. Murakami, E. Undzys, A. Aman, B. Press and S. D. Li, *Journal of controlled release : official journal of the Controlled Release Society*, 2012, **162**, 575-581.
34. W. Wei, P. P. Lv, X. M. Chen, Z. G. Yue, Q. Fu, S. Y. Liu, H. Yue and G. H. Ma, *Biomaterials*, 2013, **34**, 3912-3923.
35. Z. Wang, Y. Zhang, F. Jiang, H. Fang and Z. Wang, *Polymer Chemistry*, 2014, **5**, 3379-3388.
36. Y. Sanada, I. Akiba, K. Sakurai, K. Shiraishi, M. Yokoyama, E. Mylonas, N. Ohta, N. Yagi, Y. Shinohara and Y. Amemiya, *Journal of the American Chemical Society*, 2013, **135**, 2574-2582.
37. H. K. Patra, N. U. Khaliq, T. Romu, E. Wiechec, M. Borga, A. P. F. Turner and A. Tiwari, *Advanced Healthcare Materials*, 2014, **3**, 526-535.
38. A. Tiwari and M. Prabaharan, *Journal of Biomaterials Science, Polymer Edition*, 2010, **21**, 937-949.
39. S. K. Shukla, Nidhi, Sudha, Pooja, Namrata, Charu, Akshay, Silvi, Manisha, Rizwana, A. Bharadvaja, G. C. Dubey and A. Tiwari, *Advanced Materials Letters*, 2013, **4**, 714-719.
40. Y. Huang, J. Lu, X. Gao, J. Li, W. Zhao, M. Sun, D. B. Stolz, R. Venkataramanan, L. C. Rohan and S. Li, *Bioconjugate chemistry*, 2012, **23**, 1443-1451.
41. M. Gao, P. M. Lau and S. K. Kong, *Archives of toxicology*, 2014, **88**, 755-768.
42. Y. Zhang, S. F. Ali, E. Dervishi, Y. Xu, Z. Li, D. Casciano and A. S. Biris, *ACS Nano*, 2010, **4**, 3181-3186.
43. C. Ge, J. Du, L. Zhao, L. Wang, Y. Liu, D. Li, Y. Yang, R. Zhou, Y. Zhao, Z. Chai and C. Chen, *Proceedings of the National Academy of Sciences*, 2011, **108**, 16968-16973.
44. S. Fredenberg, M. Wahlgren, M. Reslow and A. Axelsson, *International Journal of Pharmaceutics*, 2011, **415**, 34-52.
45. O. P. Medina, N. Pillarsetty, A. Glekas, B. Punzalan, V. Longo, M. Gönen, P. Zanzonico, P. Smith-Jones and S. M. Larson, *Journal of Controlled Release*, 2011, **149**, 292-298.



BA-loaded cellulose-graft-poly(L-lactic acid) nanoparticles were fabricated by employing cellulose and poly(L-lactic acid) as materials and betulinic acid as a model drug. The nanoparticles have appropriate size and excellent antitumor activities.
250x124mm (300 x 300 DPI)